

Catalysis Science & Technology

Accepted Manuscript



This is an *Accepted Manuscript*, which has been through the Royal Society of Chemistry peer review process and has been accepted for publication.

Accepted Manuscripts are published online shortly after acceptance, before technical editing, formatting and proof reading. Using this free service, authors can make their results available to the community, in citable form, before we publish the edited article. We will replace this *Accepted Manuscript* with the edited and formatted *Advance Article* as soon as it is available.

You can find more information about *Accepted Manuscripts* in the [Information for Authors](#).

Please note that technical editing may introduce minor changes to the text and/or graphics, which may alter content. The journal's standard [Terms & Conditions](#) and the [Ethical guidelines](#) still apply. In no event shall the Royal Society of Chemistry be held responsible for any errors or omissions in this *Accepted Manuscript* or any consequences arising from the use of any information it contains.



Journal Name

ARTICLE

Enlarging the tools for efficient enzymatic polycondensation: structural and catalytic features of cutinase 1 from *Thermobifida cellulositytica*.

Received 00th January 20xx,
Accepted 00th January 20xx

DOI: 10.1039/x0xx00000x

www.rsc.org/

A. Pellis,^a V. Ferrario,^b B. Zartl,^a M. Brandauer,^c C. Gamerith,^c E. Herrero Acero,^c C. Ebert,^b L. Gardossi*,^b G. M. Guebitz^{a,c}

Cutinase 1 from *Thermobifida cellulositytica* is reported for the first time as an efficient biocatalyst in polycondensation reactions. Under thin film conditions the covalently immobilized enzyme catalyzes the synthesis of oligoesters of dimethyl adipate with different polyols leading to higher M_w (~1900) and M_n (~1000) if compared to lipase B from *Candida antarctica* or cutinase from *Humicola insolens*. Computational analysis discloses the structural features that make this enzyme readily accessible to substrates and optimally suited for covalent immobilization. As lipases and other cutinase enzymes, it presents hydrophobic superficial regions around the active site. However, molecular dynamics simulations indicate the absence of interfacial activation, similarly to what already documented for lipase B from *Candida antarctica*. Notably, cutinase from *Humicola insolens* displays a “breathing like” conformational movement, which modifies the accessibility of the active site. These observations stimulate wider experimental and bioinformatics studies aiming at a systematic comparison of functional differences between cutinases and lipases.

Introduction

The rising demand for advanced polyesters, displaying new functional properties, has boosted the development of new biocatalyzed routes for polymer synthesis, where enzymes concretely respond to the challenge of combining benign conditions with high selectivity and efficient catalysis. Enzymes are attractive sustainable alternatives to toxic catalysts used in polycondensation, such as metal catalysts and tin in particular.¹ Moreover, they enable the synthesis of functional polyesters that are otherwise not easily accessible by using traditional chemical routes because of the instability of some monomers under the elevated temperatures used in traditional approaches.² For example, it has been reported that itaconic acid (and its esters) were polymerized in the presence of different polyols leading to side-chain functionalized oligoesters, where the preserved vinyl moiety is exploitable for further functionalization.³⁻⁵ Polymeric products containing epoxy moieties have been also synthesized enzymatically.⁶ Although the size of polymers obtainable through biocatalysis might be modest,⁴ the molecular weight of oligomers can be enhanced by combining chemical or thermal methods. Hydrolases, and more specifically

Candida antarctica lipase B (CaLB), are the most widely investigated enzymes⁷⁻⁹ in ring opening polymerization (ROP) reactions and in the polycondensation of a wide array of monomers.^{2, 10}

While various immobilized-CaLB preparations have been studied and applied in polyesters synthesis, the potential of other esterases remain insufficiently explored.⁸ Besides CaLB, Gross and co-workers reported also the activity of cutinase from *Humicola insolens* (HiC) in the polycondensation of linear dicarboxylic acids and their esters (eg. adipic acid, diethyl sebacate)^{11, 12} and its application in the ring opening polymerizations of lactones (eg. ϵ -caprolactone, ω -pentadecalactone).^{13, 14} More recently, the same cutinase showed an extraordinary hydrolytic activity towards aliphatic/aromatic polyesters.¹⁵

Concerning the catalytic properties of cutinase enzymes, various fungal cutinases have been isolated and characterized¹⁶ since these enzymes are involved in plant pathologies caused by the depolymerization of cutin, a three-dimensional polymer of inter-esterified hydroxyl and epoxy-hydroxy fatty acids with chain lengths mostly between 16 and 18 carbon atoms.¹⁷ Interestingly, also pancreatic lipase has been reported to hydrolyze cutin, thereby releasing oligomers and monomers.¹⁸

The interest of cutinases as biocatalysts arises from different studies addressing their applications on unnatural substrates and in industrial processes, which include hydrolysis of milk fats, petrol manufactory, as well as production of detergents, structured triglycerides, surfactants, flavor esters, chiral pharmaceuticals and agrochemicals.¹⁹⁻²² Recently, cutinase from *Fusarium solani* pisi showed a consistent synthetic activity for the production of polyamides.^{23,24} Fungal cutinases from *Penicillium citrinum*,²⁵ *Thielavia terrestris*²⁶ or *Thermobifida* species^{27,28} have been also applied in the hydrolysis of commercial aliphatic/aromatic polyesters such as poly(lactic acid) (PLA), poly(1,4-butylene adipate-

^a University of Natural Resources and Life Sciences, Institute for Environmental Biotechnology, Konrad Lorenz Strasse 20, 3430 Tulln an der Donau, Austria.

^b Laboratory of Applied and Computational Biocatalysis, Dipartimento di Scienze Chimiche e Farmaceutiche, Università degli Studi di Trieste, Piazzale Europa 1, 34127, Trieste, Italy.

^c Austrian Centre of Industrial Biotechnology GmbH, Division Enzymes and Polymers, Konrad Lorenz Strasse 20, 3430 Tulln an der Donau, Austria.

† Footnotes relating to the title and/or authors should appear here.

Electronic Supplementary Information (ESI) available: [details of any supplementary information available should be included here]. See DOI: 10.1039/x0xx00000x

co-1,4-butylene terephthalate) (PBAT), poly(butylene succinate) (PBS) and poly(ethylene terephthalate) (PET) without affecting the bulk properties of the polymers.¹⁵

Although there are some indications of potential applications of cutinases in polymer chemistry, scientific literature is lacking from a systematic analysis of structural and functional properties of cutinases and a rationalization of differences between lipase and cutinase enzymes, on the light of the fact that they share the specificity towards highly hydrophobic substrates. Detailed studies of the crystal structure of cutinase from *Fusarium solani pisi* (Fsp)²⁹ showed that its catalytic serine is not buried into the protein core and the active site is accessible by solvents and substrates. In analogy with lipases, Fsp has mobile α -helices domains defining the active site entrance, but the enzyme does not undergo conformational changes preventing the active site accessibility.^{16,30} Notably, while the activity of most lipases is greatly improved at water-lipid interfaces, it is known that CaLB does not exhibit significant conformational modifications ascribable to interfacial activation³¹ and recent bioinformatics analysis support the idea that CaLB is functionally and structurally assimilable to esterases.³² In the present work, we introduce the cutinase 1 from *Thermobifida cellulolytica* (Thc_cut1) as a biocatalyst able to catalyze the synthesis of linear polyesters with a higher efficiency as compared to lipase B from *Candida antarctica* or cutinase from *Humicola insolens*. The latter are among the few enzymes reported so far for the synthesis of polyesters. The potential of Thc_cut1 and of some engineered mutants in the hydrolysis of PET was recently documented^{33,34} but its synthetic activity has been never explored before. The data here presented indicate that the covalently immobilized Thc_cut1 catalyzes, under solvent-less and thin film conditions,^{4,5} the synthesis of an array of linear biobased oligoesters both in solvent and bulk systems, leading to improved conversions and number average molecular weight (M_n) when compared to CaLB and HiC employed under the same conditions. A further advantage of this cutinase is represented by its structural features that enable a much higher recovery of enzymatic activity upon covalent immobilization, which is of crucial importance for practical industrial applications.³⁵ A preliminary computational study provides the first structural analysis of Thc_cut1 and tries to shed light on the different behavior of this enzyme as compared to CaLB and HiC.

Homology model of cutinase 1 from *Thermobifida cellulolytica* (Thc_cut1): preliminary structural analysis and comparison with *Humicola insolens* cutinase (HiC).

The crystal structure of *Thermobifida cellulolytica* cutinase (Thc_Cut1) has not been solved yet. Therefore, a model was constructed by homology modelling using the protein sequence from the NCBI GenBank nucleotide sequence HQ147785.³³ We use as a template the structure of *Thermobifida fusca* (PDB³⁶ code 4CG1³⁷), which shares 99.23% of sequence identity with Thc_Cut1 and differs only for residues 19 and 137 (Arg and Ser in *Thermobifida fusca* cutinase are replaced by Ser and Thr in Thc_Cut1) (Fig 1). The final 3D model of Thc_cut1 was highly reliable as indicated by a GMQE value of 0.99. The Thc_cut1 catalytic triad is constituted by Ser131, His209 and Asp177 whereas Tyr61 and Met132 form the oxyanion hole. Interestingly, although Thc_cut1 and HiC belong to the same cutinase family (E.C. 3.1.1.74), they are quite different as indicated by superimposition of the crystal structure of HiC (PDB code 4OYY)³⁸ with the 3-D model of Thc_cut1. HiC consists of a polypeptide chain of only 193 amino acids (19.89 kDa), whereas Thc_cut1 is composed by 262 amino acids (28.18 kDa). Moreover, the sequence alignment (Fig1) shows only 9% of sequence identity.

The catalytic serine (Ser105 and Ser131 for HiC and Thc_cut1 respectively) and the residues forming the oxyanion hole (Ser28, Met106 and Tyr61, Met132 for HiC and Thc_cut1 respectively) were taken as a reference for performing the structure superimposition (Fig 1c). The comparison of the two enzyme structures (Fig 1a and b) reveals that the two enzymes share a α/β hydrolase fold but the main difference is related to the location and accessibility of their active sites. While Thc_cut1 has a catalytic triad placed in a superficial and accessible groove, the active site of HiC (Ser105, His188, and Asp175) is placed in a deeper cavity.

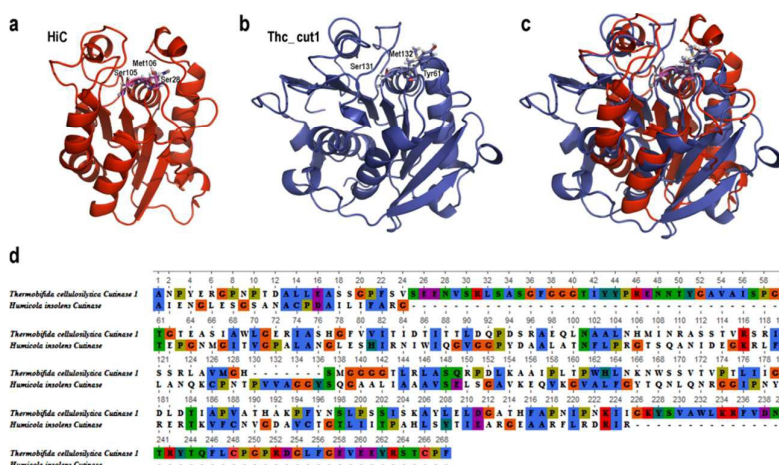


Fig 1. Representation of the three-dimensional structures of HiC (a), Thc_cut1 (b) and the two cutinase structures superimposed on the bases of their catalytic residues (c). Catalytic serines and the residues forming the oxyanion hole of each enzyme are represented in sticks mode and are labeled. Sequence alignment (d) was guided by the superimposition of residues forming the catalytic machinery. Residues are colored according to Clustal W Color scheme.

reactions.

As previously reported by our group and others, covalent immobilization is an important pre-requisite in enzymatic polycondensation.^{2,4} Obviously, a mono-molecular dispersion of the native enzyme would lead to the highest reaction rate and higher molecular weights, as largely documented in the literature.² However, contamination of reaction product with free enzyme must be avoided and recovery of the biocatalyst is mandatory for an economic process.

In the present study, the two cutinases and CaLB were immobilized on epoxy activated organic polymeric resins (EC-EP/M from Resindion S.r.l.).⁴ As reported in Table 1, more than 99% of the two cutinases and 87% of CaLB was bound onto EC-EP within the first two hours. The prompt adsorption and binding of Thc_cut1 (Fig S1 of SI) is most probably ascribable to the occurrence of hydrophobic interactions between the hydrophobic areas of the proteins and the resin, as previously reported for lipases but never documented for cutinases.⁵ Interestingly, less hydrophobic resins led to poorer results (Fig S1 of SI).

Table 1 Immobilization yields and recovered activities of different hydrolases immobilized on EC-EP epoxy-carrier using 10 mg of protein per g of dry resin in 10 mL buffer. Immobilization was performed in 0.1 M Tris-HCl buffer pH 7 at 21 °C for 24 h.

Enzyme	Bound enzyme (%) [*]	Recovered activity (%) [^]
Thc_cut1	>99	37
CaLB	87	8
HiC	>99	23

^{*} Calculated by evaluating the residual activity and protein concentration in the supernatant.

[^] Percentage of enzyme activity exhibited by the immobilized preparation when compared to the soluble form.

All results are the average of two independent immobilization procedures.

The covalently immobilized enzymes were termed iThc_cut1, iHiC and iCaLB and their hydrolytic activities were respectively of 13 ± 2 , 8 ± 1 and 17 ± 2 U g⁻¹. The two immobilized cutinases retain a much higher percentage of the original activity, especially in the case of Thc_cut1 (37%). Indeed, the poor immobilization yield observed with CaLB (8%) is in line with different studies that have already reported and commented the difficulties encountered in the efficient immobilization not only of CaLB³⁹ but also lipases from *Pseudomonas sp.*⁴⁰ and from *Candida rugosa*.⁴¹

A possible rational explanation of the higher immobilization yields of the two cutinases comes from the analysis of distribution of Lys residues on the surface of the three enzymes (Fig 2).

The primary amino group of Lys is the main candidate for the formation of covalent bonds via nucleophilic attack of epoxy functionalities.^{31,42} The Lys residues are located far from the active sites of Thc_cut1 and HiC, and this factor is expected to favor the correct orientation of the enzyme upon binding and, conversely, the accessibility of the active site (Fig 2). In contrast, two out of the nine Lys residues of CaLB are situated close to the active site.

The three hydrolases were also compared in terms of hydrophilic-hydrophobic balance of their surface. It is largely recognized that the enzyme surface properties affect not only enzyme stability⁴³ but also the efficacy of different protocols for enzyme immobilization.³¹ Lipases generally display a polarization of the hydrophilic and hydrophobic areas, in agreement with the natural evolution of these enzymes which are able to act on hydrophobic substrates. The hydrophobic side of the enzyme corresponds to the active site, which normally points towards the water-lipid interface. On that respect, Fig 3 shows that more than 50% of the surface of the two cutinases is hydrophobic, which is purposeful to the approaching and recognition of the hydrophobic cutin, their natural substrate. HiC is considerably smaller (193 aa) when compared to CaLB and Thc_cut1 (317 and 262 residues respectively). It is also evident that the active site of Thc_cut1 is the most superficial and accessible.

It is important to point out that CaLB is expressed in *Aspergillus sp.* and the analysis of the primary sequence of CaLB indicates the presence of a N-glycosylation site at Asn 74. As previously reported, the glycan masks an hydrophobic spot on CaLB surface.³⁹ Consequently, the overall hydrophobicity of glycosylated CaLB is comparable to Thc_cut1, which is expressed in *E. coli* and is not glycosylated. This observation is also in agreement with the high affinity of Thc_cut1 for the hydrophobic EC-EP carrier (Table 1).³⁹

All polycondensation reactions were carried out using enzymatic preparations with a water content below 0.1% w w⁻¹ in order to avoid competing hydrolytic reactions. The stability of the immobilized enzymes was investigated in terms of protein detachment from the support and resulted to be less than 2%. Indeed, it is known that magnetic and mechanical mixing are responsible for damage of carriers and thin-film reactors have already demonstrated to preserve the integrity of EC-EP resins while overcoming the viscosity of solvent-less polycondensations.^{4,42,44}

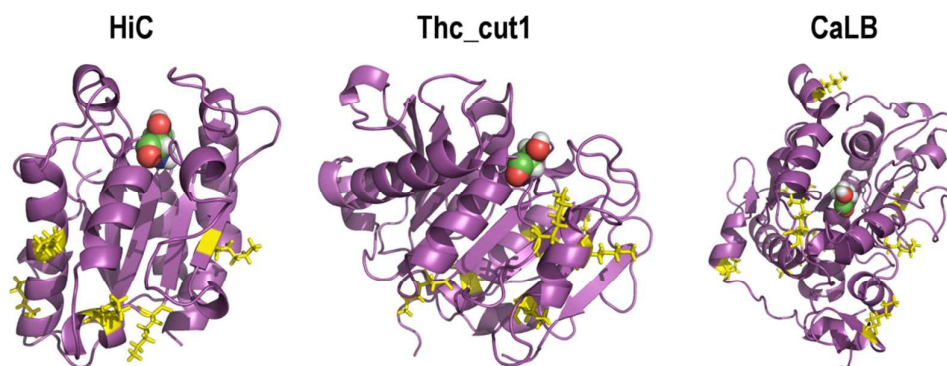


Fig 2. Lysine residues on the surface of the three hydrolases, highlighted in yellow sticks mode. The catalytic Ser of each enzyme is represented in sphere mode.

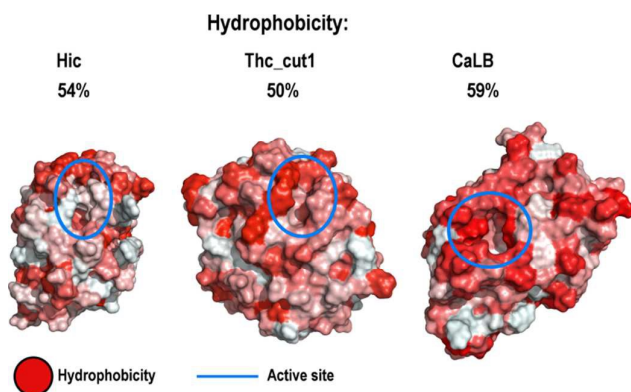


Fig 3. Comparison of the hydrophobicity of the surface of the three hydrolases. The openings of the active sites are highlighted within cyan circles. The extent of the surface hydrophobicity of the three enzymes was calculated and represented by using the color_h script of the PyMOL software.

Comparison of Thc_cut1, HiC and CaLB in the polycondensation of DMA with BDO.

In order to compare the behavior of the three enzymes, a model reaction between dimethyl adipate (DMA) and 1,4-butanediol (BDO) was investigated. These monomers are widely used in polymer synthesis and their biobased production gained further interest in the recent years. Polycondensations were conducted using a thin-film solvent-free system⁵ at 70 °C and 100 kPa (Table 2).¹¹ The investigation included also Novozym[®] 435, the enzymatic preparation most widely used in polycondensations, although it has been demonstrated that it causes protein contamination and it does not allow an efficient recycling.⁴

Table 2 Polycondensation of DMA with BDO by different hydrolases at 24 h at 70 °C and 100 kPa, using 10% w⁻¹ of biocatalyst.

Enzymatic preparation	Conversion (%) ^A	M _w	M _n	PD
Novozym [®] 435	78	1040	561	1.85
iCaLB	76	888	528	1.68
iThc_cut1	86	1923	985	1.95
iHiC	-	-	-	-

^A Calculated via ¹H-NMR by comparing the ratio between the polyol methylene groups adjacent to -OH area (B₁) and the internal methylene groups area of DMA (A₁, assumed as constant). All reactions were performed in duplicates.

^{*} Calculated via GPC calibrated with low molecular weight polystyrene standards ranging from 250-70000 Da.

Interestingly, the polycondensation catalyzed by iThc_cut1 led to the highest monomer conversion (86% calculated by ¹H-NMR analysis) with reaction products reaching a M_w of 1923 Da (Fig S2-S4 in SI). The data appears quite promising when considered that the commercial Novozym[®] 435 gave 78% monomer conversion with M_w of 1040 Da (Fig S5-S7 in SI) notwithstanding previous studies documented the tendency of such formulation to release part of the free enzyme in the reaction mixture.⁴

Regarding the use of HiC, Hunsen et al. claimed that the covalently immobilized enzyme was able to catalyze the polycondensation of adipic acid with C₄, C₆ and C₈ linear polyols in solvent-less condition at 70 °C and 10 mm Hg (about 1.3 kPa).¹² Our attempts to synthesize similar polyesters starting from dimethyl ester, although at 100 kPa, gave no observable product even when the free HiC enzyme was employed. Monomer conversions of around 10% were obtained only using adipic acid as monomer.

It must be underlined that polyesters of much higher M_w were reported in studies employing adsorbed CaLB (e.g. Novozym[®] 435) in polycondensation of structurally different monomers.² Nevertheless, in the present study our interest was mainly focused on esters of adipic acid and BDO as they are bio-based monomers available at industrial scale. Previous studies^{45,46} indicated that these short chain monomers led to polyesters with M_w in the range of 600-2200 Da. However, in such cases the detachment of the native enzyme was observed and its dispersion in the reaction mixture. As recently demonstrated, the fine and homogeneous distribution of the biocatalyst affects the elongation of polymers much more than the specific activity of the biocatalyst.⁵ Therefore, in the case of Novozym[®] 435, polycondensation is catalyzed both by the immobilized iocatalyst and by the fraction of native CaLB dispersed in the reaction mixture and that favor the chain elongation.⁴

Taken these factors into account, it is noteworthy that the size of oligoesters here reported is of the same order of magnitude of products previously obtained using different formulations of CaLB for the polycondensation of similar monomers.^{4,5,44}

The results obtained in the study of the biocatalyst recyclability (Fig 4) demonstrate that by using a thin-film reaction system and solvent-less conditions the covalently immobilized Thc_cut1 retains most of its activity after 10 synthetic cycles. Details of time course are available in ESI, Fig S8.

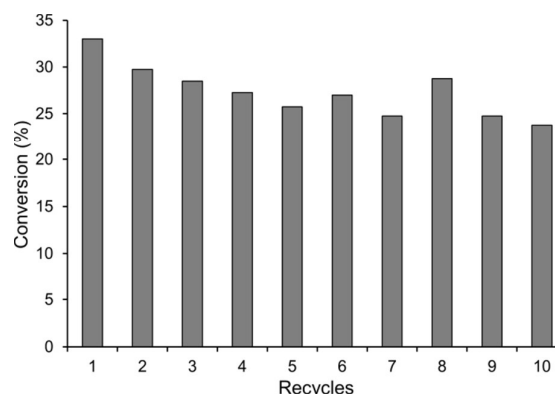


Fig 4. Evaluation of the recyclability of the Thc_cut1 covalent preparation over 10 cycles expressed as a percentage of the BDO monomer reacted after 4 h of reaction.

It must be underlined that our previous studies demonstrated already the recyclability of covalently immobilized CaLB using the same reaction conditions, whereas Novozym[®] 435 undergoes a progressive detachment of the enzyme and a decrease of enzymatic activity.⁴

Experimental data, combined with computational information, indicate that Thc_cut1 is a promising biocatalyst for applications in polycondensation reactions and it is particularly suitable for being covalently immobilized on EC-EP carriers. Moreover, the stability of the enzyme preparations can be of industrial interest in the view of an up scaling of the process.

Polycondensation of dimethyl adipate catalyzed by iThc_cut1 using different diols.

In order to assess the substrate specificities of iThc_cut1 towards different monomers, a set of qualitative screening reactions was carried out using DMA and diols with different chain-lengths (C₂-C₁₂). These preliminary tests were carried out in bulk and monitored

by means of $^1\text{H-NMR}$. They indicated that *iThc_cut1* is able to catalyze the polycondensation of DMA with BDO, HDO, ODO and DDO (Table 3). The production of short chain oligoesters was demonstrated by ESI-MS. After 24 h, the longest reaction product was an 8 units oligomer obtained in the reaction between DMA and BDO while the most abundant products were trimers, tetramers and pentamers in all the performed reactions (Fig S9 in SI). Further quantitative information on the efficiency of *iThc_cut1* was obtained by studying the time-course of the polycondensation of DMA with C_4 , C_6 and C_8 linear diols using a thin-film reaction system at environmental pressure and in solvent-free conditions (Fig 4).⁴⁷

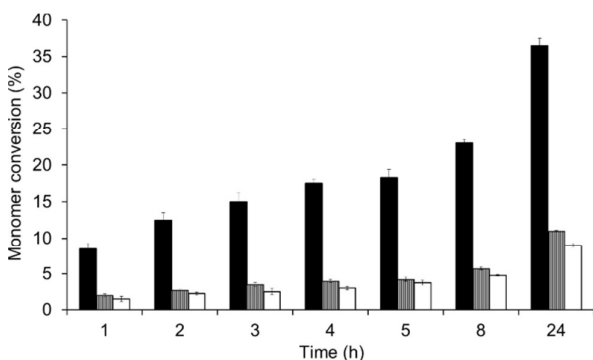


Fig 5. Time-course of the solvent-free polycondensation of DMA with BDO (black bars), HDO (stripe bars) and ODO (white bars) catalyzed by immobilized *Thc_cut1* having a hydrolytic activity of 7 U g^{-1} . Monomer conversion was calculated via $^1\text{H-NMR}$. All reactions were performed in duplicates. It must be noted that these reactions were catalyzed by an enzyme preparation displaying a much lower activity ($7 \pm 2 \text{ U g}^{-1}$) in order to allow suitable monitoring of the polycondensation reaction time course while maintaining the same monomer-biocatalyst ratio ($10\% \text{ w w}^{-1}$).

From Fig 5 it appears that *Thc_cut1* is more efficient in the polycondensation of C_4 diol leading to 37% of monomer conversion in 24 h while the C_6 and the C_8 dialcohols were converted only by 11% and 9% respectively. However, the observed rate of conversion may be ascribed not only to different enzyme specificity but also to different viscosity of the reaction systems under solvent-less conditions. Indeed, while BDO is a liquid, the other polyols are solid

Table 4 Polycondensation of DMA with C_4 , C_6 and C_8 linear polyols at 24 h catalyzed at 70°C and 100 mPa in toluene using $10\% \text{ w w}^{-1}$ *iThc_cut1* with a hydrolytic activity of 13 U g^{-1} .

Linear Polyol	Conversion (%) ^A	M_w^*	M_n^*	PD [*]
BDO	50	435	400	1.09
HDO	52	440	453	1.17
ODO	55	551	465	1.19

^A Calculated via $^1\text{H-NMR}$ by comparing the ratio between the polyol methylene groups adjacent to -OH area (B_1) and the internal methylene groups area of DMA (A_1 , assumed as constant). All reactions were performed in duplicates.

^{*} Calculated via GPC calibrated with low molecular weight polystyrene standards 250-70000 Da.

at 25°C and they are simply dispersed in DMA before heating at 70°C to obtain a homogeneous phase. The possible effect of viscosity and mass transfer on data in Fig 5 was confirmed by carrying out the polycondensation in two different organic solvents, namely toluene and tetrahydrofuran (THF). It has been already reported that HiC is active in several organic solvents while there are no respective data on *Thc_cut1*. The reactions were carried out by solubilizing the monomers in organic solvent at a concentration of 0.2 M and Table 4 reports the results obtained in toluene, since no polymerization product was observed using THF. The

polycondensation of DMA with C_4 , C_6 and C_8 linear polyols led to monomers conversions ranging from 50 to 55% after 24 h of reaction with M_w distributions of 400-450 Da.

It must be underlined that the activity of *Thc_cut1* in the polycondensation of BDO and dimethyl adipate opens interesting perspectives for the enzymatic synthesis of polyesters. Gross and co-workers reported that cutinase from *Humicola insolens* accepts preferably C_6 and C_8 diols in the polymerization with adipic acid while the C_4 diol is scarcely converted.¹² Moreover, previous studies reported also that HiC accepts preferably C_{10} and C_{13} diacids, while only slight activity was detected for substrates with a $<\text{C}_{10}$ carbon chain.¹¹ The same work also documented that CaLB catalyzes the polycondensation of C_3 - C_8 linear polyols with sebacic acid at 70°C in bulk, although the study did not report information on the rate of conversion of monomers but only the increase of the M_n over time.¹¹

The time course of Fig 6 shows how *Thc_cut1* converts the linear diols in toluene with similar efficiency, thus confirming a possible effect of viscosity and mass transfer in conversions reported in Table 3 and Fig 5. However, some solvent effect on the conformation and accessibility of the enzyme cannot be excluded.

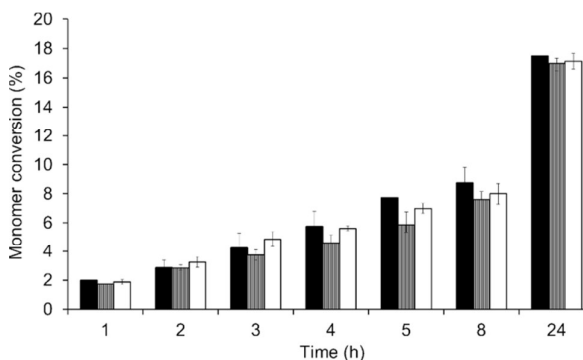


Fig 6. Time-course of the polycondensation of DMA with BDO (black bars), HDO (stripe bars) and ODO (white bars) in toluene. The reactions were catalyzed by immobilized *Thc_cut1* displaying lower activity ($7 \pm 2 \text{ U g}^{-1}$) in order to facilitate the monitoring of the polycondensation while maintaining the same monomer-biocatalyst ratio ($10\% \text{ w w}^{-1}$). Monomer conversion was calculated via $^1\text{H-NMR}$. All reactions were performed in duplicates.

Comparison of dynamic behavior of *Thc_cut1*, HiC, and CaLB in different media.

In order to investigate possible solvent effects on the accessibility of *Thc_cut1*, a conformational analysis was carried out by running MD

Table 3 Polyesterification of DMA with EG, PDO, BDO, HDO, ODO and DDO catalyzed by $10\% \text{ w w}^{-1}$ *iThc_cut1* with a hydrolytic activity of 13 U g^{-1} for 24 h.

Dicarboxylic acid (A)	Polyol (B)	Area -CH ₂ -OCO- (B_1) [*]	Area -CH ₂ -CO- (A_1) [*]	Monomer conversion (%) [*]
DMA	EG	X	4.0	X
	PDO	X	4.0	X
	BDO	1.79	4.0	45
	HDO	1.49	4.0	37
	ODO	1.36	4.0	34
	DDO	1.04	4.0	26

^{*} Calculated via $^1\text{H-NMR}$ by comparing the ratio between the polyol methylene groups adjacent to -OH area (B_1) and the internal methylene groups area of DMA (A_1 , assumed as constant). All reactions were performed in duplicates.

simulations for 10 ns at 343 K in explicit toluene. HiC and CaLB were also included in the study. Fig S10 in SI reports a comparison of the

starting structures (crystals for HiC and CaLB, homology model for Thc_cut1) and the conformations obtained after 10 ns of MD simulation in toluene.

Root Mean Square Fluctuation (RMSF) were calculated for each simulated protein³¹ to identify the most flexible domains (Fig 7). The analysis pointed out two very mobile domains overlooking the catalytic Ser105 of HiC, so that after 10 ns simulations in toluene the active site of HiC increases its accessibility and it assumes the shape of an open “chasm”. This observation might suggest that HiC has a behavior similar to lipases, members of the same serine-hydrolase superfamily, which are undergo dynamic opening and activation when exposed to hydrophobic phases, as a result of the movements of the flexible domains referred as “lid”.³¹

As widely known, CaLB is not characterized by the interfacial activation phenomena. This is confirmed by the RMSF analysis of Fig 7, which indicates the presence of a domain endowed with modest flexibility in the proximity of the opening of the active site corresponding to a small putative lid unable to close the active site.³¹

In Thc_cut1 the regions surrounding the opening of the active sites appear of scarce mobility, while there are terminal loops undergoing wider fluctuations. Conversely, the superficial and groove shaped active site of Thc_cut1 undergoes very limited conformational modifications in toluene (Fig S10 in ESI).

domain overlooking the active site. Although this feature is shared by most lipase enzymes, the MD simulations indicate that the active site of HiC remains open and accessible both in water and in hydrophobic environment. Nevertheless, the crystal structure shows how the putative “lid” is indeed able to assume conformations that reduce the active site accessibility in the presence of a hydrophobic inhibitor.

Of course, this behavior deserves further investigations and bioinformatics analysis to understand structural and functional differences between cutinases and lipases.

The hydrophobic surface appears to be a common feature of lipases and cutinases but it must be noted that very few studies address the differences between lipases and cutinases. Some pioneering studies indicated that cutinase enzymes are able to hydrolyze fatty acid esters and emulsified triacylglycerol as efficiently as lipases, but without any interfacial activation.^{48, 49} Structural and computational investigations of cutinase from *Fusarium solani* pisi documented that the loops surrounding the catalytic site are highly flexible.³⁰ The same studies also indicated that the absence of any significant structural rearrangements upon binding to non-hydrolyzable substrates represents an important feature of cutinase. Notably, this feature is shared by *Candida antarctica* lipase B.⁵⁰

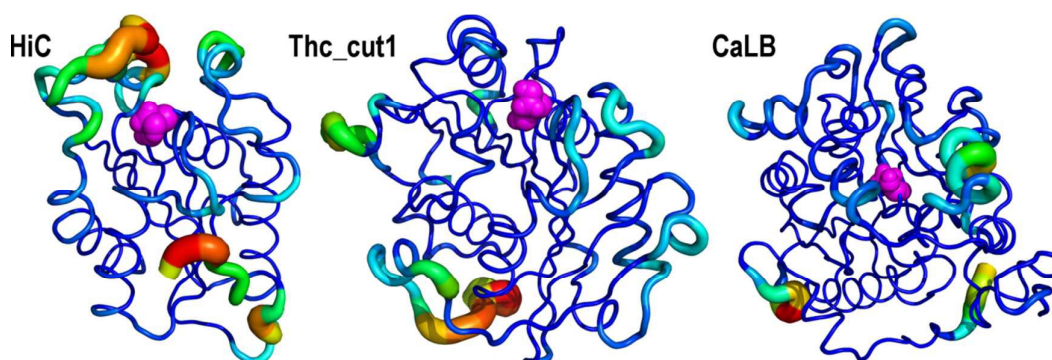


Fig 7. Representation of RMSF on the 3D structures of the three hydrolases. The thickness and “color temperature” (from blue to red) are correlated with the fluctuation observed during the 10 ns MD simulations in explicit toluene at 343 K. The thicker and red regions correspond to the highest RMSF values. The catalytic serine of each enzyme is highlighted in pink sphere mode.

In order to shed light to this lipase-like conformational behavior of HiC, further dynamic simulations were run in explicit water. Our previous studies illustrated how a number of different lipases in explicit water undergo a sort of “closure” of the active sites with a restriction of their accessibility. On the contrary, the conformation of HiC after 10 ns simulation in explicit water at 343 K becomes open and the active site is fully accessible. Quantitative details of the amplitude of the movements of domains overlooking the catalytic serine can be observed in Fig 8b, where it appears clear that the crystal structure of HiC is the less accessible. Interestingly, this structure corresponds to the crystal obtained in the presence of a hydrophobic inhibitor (diethyl-p-nitrophenyl-phosphate). No significant conformational variations were observed for CaLB and Thc_cut1 in explicit water.

Overall, this computational analysis indicates that HiC and Thc_cut1 are considerably different in terms of structure and conformational behavior. HiC presents highly mobile domains and a kind of “lid”

Other investigations reported that the atoms involved in cutinase oxyanion hole formation do not move upon inhibitor binding whereas significant displacements occur in *Rhizomucor miehei* lipase and human pancreatic lipase upon inhibition.⁵¹

The present study indicates that there is no unified picture for illustrating structural and conformational properties of all cutinases. The negligible conformational mobility of Thc_cut1 is indeed comparable with the CaLB behavior whereas the conformational modifications occurring in HiC are compatible with a “brief-like” motion able to modulate the access to the hydrophobic active site.

On the light of these preliminary evidences, a comprehensive future computational and bioinformatic comparison could elucidate the structure function relationships of these interesting enzymes in more detail.

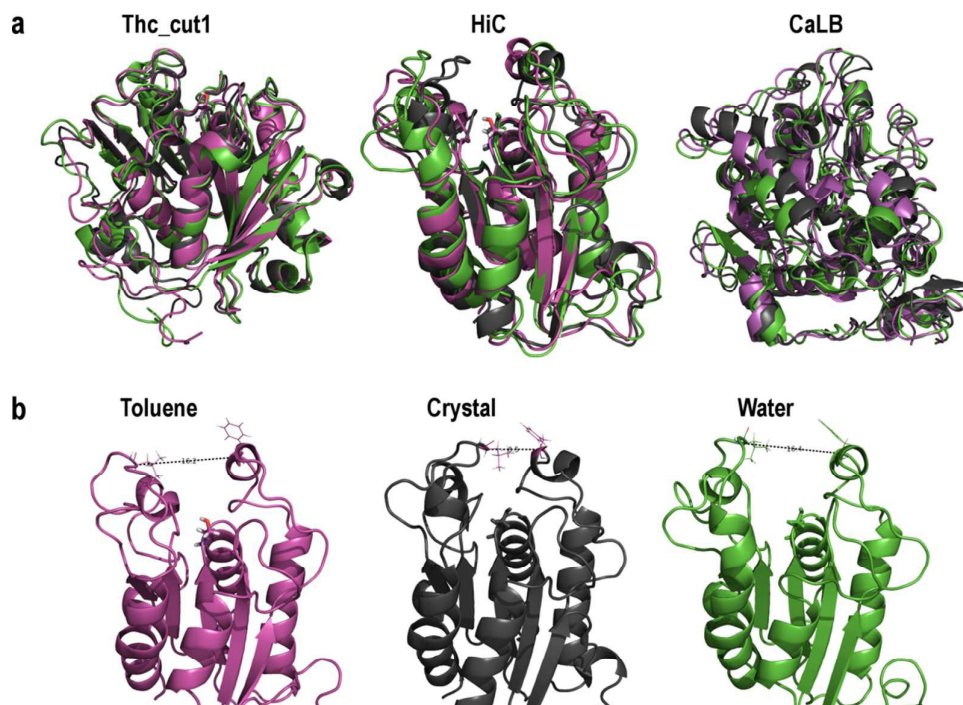


Fig 8. A: Superimposition of structures of Thc_cut1 (homology model), HiC and CaLB (crystals) with conformations obtained after MD simulations at 343 K. Legend: gray = starting 3D structure; pink = after 10 ns MD in toluene; green = after 10 ns MD in water. B: Comparison of the accessibility of HiC active site expressed as the distance between C α of Phe 70 and Lys 167. Pink (toluene) = 16.2 Å; grey (crystal structure after removal of inhibitor) = 8.5 Å; green (water) = 16.4 Å.

Conclusions

The urgency of more sustainable, selective and efficient routes for the synthesis of new generation polyesters was addressed by introducing cutinase 1 from *Thermobifida cellulolytica* (Thc_cut1) as new enzyme suitable for polycondensation reactions.

The disclosure of some methodological problems hampering the polycondensation procedures used so far (unsuitability of adsorbed immobilized biocatalysts as well as of batch reactors) motivated an integrated study addressing both the biocatalyst and the reaction system, aiming at contributing to a more rational optimization of *in vitro* enzymatic synthesis of polyesters. Covalently immobilized Thc_cut1 catalyzes, under thin film conditions,^{4,5} the synthesis of an array of linear biobased oligoesters both in solvent and bulk systems, leading to improved conversions and M_n when compared to lipase B from *Candida antarctica* (CaLB) and cutinase from *Humicola insolens* (HiC) employed under the same conditions. A further advantage of this cutinase is represented by its structural features enabling a much higher recovery of enzymatic activity upon covalent immobilization, which is of crucial importance for practical industrial applications.³⁵ Preliminary computational studies provide the first structural analysis of Thc_cut1 and shed light on the different conformational behavior of this enzyme as compared to CaLB and HiC. Structural analyses indicate that Thc_cut1 has a very superficial and fully accessible active site both in aqueous and hydrophobic media. Interestingly, Thc_cut1 shares some structural and conformational properties with lipase B from *Candida antarctica*, whereas cutinase from *Humicola insolens* has highly mobile domains able to modify the accessibility of its active

site. Such remarkably different behavior of these two cutinases motivate further comprehensive bioinformatics analysis able to elucidate structural and functional differences among cutinases and lipases, two enzyme classes sharing highly hydrophobic surfaces and the ability to hydrolyze insoluble substrates.

Experimental section

Chemicals and reagents.

EC-EP/M and EC-HFA/M Sepabeads were kindly donated by Resindion S.r.l., (Mitsubishi Chemical Corporation, Milan, Italy). EC-EP/M beads have average pore diameter of 10–20 nm, particle size in the range of 200–500 μm and water retention around 55–65%. Dimethyl adipate (DMA), ethylene glycol (EG) and 1,2-propanediol (PDO) were purchased from Sigma-Aldrich. 1,4-butanediol (BDO), 1,6-hexanediol (HDO), 1,8-octanediol (ODO) and 1,12-dodecanediol (DDO) were purchased from Merck. All other chemicals and solvents were also purchased from Sigma-Aldrich at reagent grade, and used without further purification if not otherwise specified.

Enzymes.

The recombinant *Thermobifida cellulosilytica* cutinase 1 (Thc_cut1) was produced and purified as previously described. The organism used for the expression was *E. Coli*.³³ Novozym[®] 435 was purchased from Sigma-Aldrich (product code: L4777) containing *Candida antarctica* lipase B immobilized on macroporous acrylic resin with a specific activity of $>5000 \text{ U g}^{-1}$ (PLU Units, determined by producer). Lypozyme CaLB (protein concentration of 8 mg mL^{-1}) was a kind gift from Novozymes (DK). The cutinase from *Humicola insolens* (HiC) (protein concentration of 11.2 mg mL^{-1}) was a gift from Novozymes (Beijing, China) and was purified as previously described¹⁵ prior to use.

Activity assay for native lipase and cutinases.

Activity was measured at 21°C using *p*-nitrophenyl butyrate (PNPB) as a substrate as previously reported by Ribitsch et al. with some modification.²⁷ PNPB was selected because lipases and cutinases display different substrate specificity and a general test for esterase activity was preferred rather than the typical tributyrin hydrolysis assay. In any case, no direct comparison between lipase and cutinase activity was reported. The final assay mixture was made up of 200 μL of solution B and 20 μL of enzyme solution (solution A: 86 μL of PNPB and 1000 μL of 2-methyl-2-butanol; solution B: 40 μL of solution A and 1 mL of 100 mM Tris-HCl buffer at pH 7). The increase of the absorbance at 405 nm due to the hydrolytic release of *p*-nitrophenol ($\epsilon_{405 \text{ nm}} = 9.36 \text{ mL } (\mu\text{mol cm})^{-1}$) was measured over time using a Tecan plate reader using plastic 96 well plates. A blank was included using 20 μL of buffer instead of enzymatic solution. The activity was calculated in units (U), where 1 unit is defined as the amount of enzyme required to hydrolyze 1 μmol of substrate per minute under the given assay conditions.

Activity assay for immobilized enzymes.

Activity was measured at 21°C using PNPB as substrate. The final assay mixture was made up of 0.1 mL of the substrate solution (86 μL of PNPB and 1000 μL of 2-methyl-2-butanol), 11 mL of 100 mM Tris-HCl buffer at pH 7 and 20 mg of

immobilized enzyme preparation. The increase of the absorbance at 405 nm due to the hydrolytic release of *p*-nitrophenol ($\epsilon_{405 \text{ nm}} = 9.36 \text{ mL } (\mu\text{mol cm})^{-1}$) was measured over time with a HACH Lange benchtop spectrophotometer using plastic cuvettes. A blank was included using beads where glycine was used instead of enzyme as blocker for the epoxy-activated beads. The activity was calculated in units (U), where 1 unit is defined as the amount of enzyme required to hydrolyze 1 μmol of substrate per minute under the given assay conditions.

Evaluation of enzyme leaching.

Immobilized enzyme preparations were incubated as described above without adding the PNPB solution. Samples were taken after 5, 10, 15 and 30 min and the biocatalyst was removed via filtration. The substrate solution was added to the supernatant and the residual esterase activity was assessed as described above.

Protein quantification.

Protein concentrations were determined by using the BioRad protein assay (Bio-Rad Laboratories GmbH, Vienna, Cat.No: 500-0006). Briefly, 10 μL of the sample was added into the wells of a 96-well micro-titer plate (Greiner 96 Flat Bottom Transparent Polystyrene). As soon as all the samples were placed into the wells, 200 μL of the prepared BioRad reaction solution were added to the wells (BioRad Reagent diluted 1:5 with mQH_2O). The plate was incubated for 5 min at 21°C and 400 rpm. The buffer for protein dilution (0.1 M Tris-HCl pH 7) was used as blank and BSA (bovine serum albumin) as standard. The absorption after 5 min was measured at $\lambda = 595 \text{ nm}$ and the concentration calculated from the average of triplicate samples and blanks.

Immobilization of Thc_cut1, HiC and CaLB on epoxy-activated beads.

The epoxy-activated beads were washed with ethanol (2 times) and double distilled H_2O (2 times) prior to use. A total of 1.0 g of dry epoxy-activated beads were suspended in 10 mL of 1 mg mL^{-1} enzyme solution in 0.1 M Tris-HCl buffer pH 7 at 21°C for 24 h on a blood rotator. Samples were withdrawn over time. The progress of the immobilization was monitored by evaluating the residual activity and protein concentration in the supernatant and data are reported in Fig S1 of ESI. It must be noted that Tris-HCl buffer was selected as immobilization medium because native Thc_cut1 was produced in this same buffer and the exchange of buffer would cause a loss of enzymatic activity (data not shown). After the immobilization, the enzyme preparations were extensively washed with 0.1 M Tris-HCl buffer pH 7 in order to remove all the non-covalently bound protein adsorbed on the support. Finally, in order to block the unreacted epoxy groups, the enzymatic preparations were incubated in 45 mL of 3 M glycine for 24 h at 21°C as previously reported.⁵² The enzyme preparations were extensively washed with 0.1 M Tris-HCl buffer pH 7 and dried for 48 h at 30°C under reduced pressure (13.3 kPa) in a desiccator containing silica gel prior to use (if not otherwise specified). The immobilized preparations are termed iThc_cut1, iCaLB and iHiC, respectively.

Moisture determination.

0.2 g of immobilized enzymatic preparation was weighted in a tarred weighting bottle (A), dried for 6 h at 120 ± 5 °C, cooled down in a dessicator until constant weight was reached and weighted again (B). The moisture content was calculated as follows:

$$\text{Moisture content (\%)} = [(A-B)/A] \times 100$$

A table with the calculated water content of the immobilized preparations can be found in ESI (Table S1). All determinations were conducted in duplicates.

Enzymatic polycondensation of DMA e BDO using a thin-film reaction system under solventless conditions.

6.0 mmol A and 6.0 mmol B and the biocatalysts iThc_cut1, iCaLB, iHiC or Novozym® 435 (10% w w⁻¹ respect to the total amount of monomers) were incubated in a 50 mL round bottom flask connected to a rotary evaporator at 70 °C and 100 kPa for 24 h. The molar ratio of A and B was 1.0:1.0. During the polymerization process the biphasic system became a monophasic homogeneous transparent solution. The final product was a viscous sticky colorless liquid which was solubilized in DCM. After solvent evaporation, the crude product was analyzed by GPC, ESI-MS and ¹H-NMR without any further purification. All reactions were performed in duplicates and compared to a control without enzyme.

Screening of activity of iThc_cut1 in the polycondensation of dimethyl adipate (A) and diols with different chain length (B).

A fast preliminary screening of the substrate specificity of Thc_cut1 towards different diols was performed by incubating 5.0 mmol of A, 5.0 mmol of B and iThc_cut1 (10% w w⁻¹ respect to the total amount of monomers). These qualitative preliminary tests were carried out using common 4-mL reaction vials at atmospheric pressure and 70 °C and applying magnetic stirring for 24h. The molar ratio of A and B used was 1.0:1.0. During the polymerization process the initial biphasic system became a monophasic homogeneous transparent solution. The final products were solubilized in tetrahydrofuran (THF) and filtered in order to remove the biocatalyst. After solvent evaporation, the crude products were analyzed by gel permeation chromatography (GPC), Electrospray Ionization-Mass analysis (ESI-MS) and proton nuclear magnetic resonance spectroscopy (¹H-NMR) without any further purification. All reactions were performed in duplicates and compared to a control without enzyme. The same protocol was applied for the reactions conducted in organic solvent using 12-mL reaction vials and a concentration of monomers of 0.2 M.

GPC.

Samples were dissolved in THF (250 ppm BHT as inhibitor) and filtered through filter paper (595 ½, Whatman GmbH, Dassel, Germany). In case of liquid samples, the starting solvent was removed under reduced pressure. Gel permeation chromatography was carried out at 30 °C on an Agilent Technologies HPLC System (Agilent Technologies 1260 Infinity) connected to a 17369 6.0 mm ID x 40 mm L H_{HR}-H, 5 µm Guard column and a 18055 7.8 mm ID x 300 mm L GMH_{HR}-N, 5 µm TSKgel liquid chromatography column (Tosoh Bioscience, Tessenderlo, Belgium) using THF (250 ppm BHT as inhibitor) as eluent (at a flow rate of 1 mL min⁻¹). An Agilent Technologies G1362A refractive index detector was employed for detection.

The molecular weights of the polymers were calculated using linear polystyrene calibration standards (250-70000 Da).

¹H-NMR.

Nuclear magnetic resonance ¹H and ¹³C measurements were performed on a Bruker Avance II 400 spectrometer (resonance frequencies 400.13 MHz for ¹H) equipped with a 5 mm observe broadband probe head (BBFO) with z-gradients. CDCl₃ was used as NMR solvent if not otherwise specified.

Electrospray Ionization Mass Spectrometry (ESI-MS).

The crude reaction mixtures were analyzed on Esquire 4000 (Bruker) electrospray positive ionization by generating the ions in an acidic environment. Around 10 mg of sample was dissolved in 2 mL of methanol containing 0.1% v v⁻¹ formic acid. The generated ions were positively charged with m z⁻¹ ratio falls in the range of 200-1000. The subsequent process of deconvolution allows the reconstruction of the mass peaks of the chemical species derived from the analysis of the peaks generated.

Recyclability of Thc_cut1: polycondensation between DMA and BDO.

The recyclability study was carried out on a scale of 1.5 mL (1.6 g of monomers) according to the following procedure: DMA (1.0451 g, 6.0 mmol) and BDO (0.5407 g, 6.0 mmol, molar ratio 1.0:1.0) were mixed in a 50-mL round-bottom flask. The two monomers are liquid and completely miscible. The addition of the biocatalyst (0.1586 g of Thc_cut1, 10% w w⁻¹ respect to the total amount of monomers) started the reaction, which run for 4 h at 50 °C under atmospheric pressure (100 kPa) in the flask connected to a rotary evaporator. The conversion of DMA was monitored at 1, 2, 3 and 4 h by withdrawing volumes (about 50 µL) of the fluid crude reaction mixture that were dissolved in CDCl₃ and analyzed by ¹H-NMR.

The products and the unreacted monomers were sufficiently fluid to be filtered under reduced pressure without any addition of solvent. The immobilized biocatalyst (beads diameter 200-500 µm) was fully recovered at the end of the reaction by means of a sintered glass filter, equipped with cellulose filters. The biocatalyst was not rinsed in order to prevent any detrimental effects of solvent treatments. The recovered biocatalyst was employed for the following synthetic cycles under the conditions above described by adding the same amount of fresh monomers. It was also verified that no reaction occurred in the absence of enzyme.

Construction and analysis of the homology model of Thc_cut1.

The *Thermobifida cellulosilytica* cutinase 1 (Thc_cut1) protein sequence was taken from the NCBI GenBank nucleotide sequence HQ147785.³³ The translated protein sequence was used as input for building a homology model of the Thc_cut1 3D structure using the SWISS-MODEL server.⁵³ As a template the structure of cutinase from *Thermobifida fusca* was used (PDB³⁶ code 4CG1).³⁷ The two enzymes share high homology and differ in just two amino acids. The catalytic triad and the oxyanion hole were individuated by visual inspection taking as a reference the organization of other serine-hydrolases.³²

The final 3D structure of Thc_cut1 was obtained by SWISS-MODEL server⁵³ and evaluated by means of GMQE with a value of 0.99 (GMQE is a scoring function for homology model quality evaluation; it assumes values between 0 and 1 where higher numbers indicate higher model reliability). The final 3D structure is available in ESI (Structure Thc_cut1).

Structural and sequence comparisons.

Structure comparisons of cutinase from *Humicola insolens* (HiC) and cutinase 1 from *Thermobifida cellulosilytica* (Thc_cut1) were performed by the software PyMOL (The PyMOL Molecular Graphics System, Version 1.5.0.4 Schrödinger, LLC). 3D-structure of Thc_cut1 was generated by homology model as previously indicated; HiC crystal structure 4OYY (crystal obtained in 0.1 M Tris-HCl pH 8.5, 50 mM lysine, PEG MME 2K 11% v/v of 50% w/v stock solutions in the presence of diethyl-p-nitrophenyl-phosphate as inhibitor)³⁸ was taken from Protein Data Bank (PDB).³⁶ Structural superimposition was performed by considering catalytic residues as a reference: the catalytic serine (Ser105 and Ser131 for HiC and Thc_cut1 respectively) and the residues forming the oxyanion hole (Ser28, Met106 and Tyr61, Met132 for HiC and Thc_cut1 respectively). Subsequently, the structural superimposition was used as a reference for the sequence alignment of the two cutinases. Sequence alignment was visualized by the software UGENE;⁵⁴ aligned residues are colored according to Clustal W color scheme.⁵⁵

Surface analysis.

The representation and the calculation of the hydrophobic enzyme surfaces were performed by the color_h python script⁵⁶ for the software PyMOL. Protein structures were visualized and recorded using the PyMOL software. The 3D-structures used for the hydrophobicity comparisons were retrieved from the PDB with the code 4OYY³⁸ for HiC and 1TCA⁵⁷ for CalB, whereas the homology model was used for Thc_cut1.

Molecular dynamics simulations.

The structure of HiC 4OYY³⁸ was taken from PDB and used as starting point for the MD simulation after removal of the inhibitor diethyl-p-nitrophenyl-phosphate. The 1TCA⁵⁵ crystallographic structure was used for computing for CalB (crystal obtained in acetate buffer 20 mM pH 3.6, 20% polyethylene glycol 4000, 10% isopropanol). The Thc_Cut1 structure was obtained by homology modeling as described above. Both HiC and CalB starting structure contains just one protein molecule and the crystal water, whereas concerning the Thc_Cut1 structure, crystal water was retrieved from the 4CG1 template structure. The protonation state was calculated at pH 7.0 using the PDB2PQR server⁵⁶ based on the software PROPKA.⁵⁷ Subsequently, each protonated enzyme structure, together with its crystal water, was defined according to OPLS force field,⁵⁸ inserted in a cubic box of 216 nm³ and solvated with explicit solvent (either TIP4 water or toluene as defined by literature).⁵⁹ Thus, each enzyme system was minimized using the software GROMACS version 4⁶⁰ using a steepest descent algorithm for 10000 steps. Afterwards, equilibration MD simulations were performed with the software GROMACS version 4 for 5 ns at 343 K in an NVT environment keeping enzymes position restrained, thus allowing the equilibration of the solvent particles (toluene and

crystal water); Particle Mesh Ewald (PME) algorithm⁶¹ for the calculation of electrostatic interactions was employed, v-rescale algorithm⁶² for temperature and Berendsen algorithm⁶³ for pressure were also employed. Finally, after the removal of the every restraint on protein position, each enzyme was simulated for 10 ns at 343 K in NVT environment using the same parameters as before.

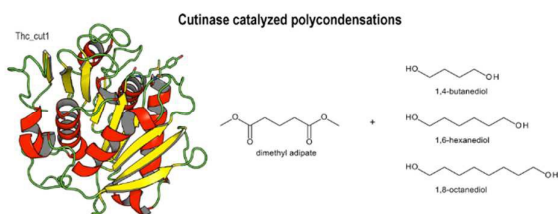
Acknowledgements

This project (Alessandro Pellis) has received funding from the European Union's Seventh Framework Programme for research, technological development and demonstration under grant agreement N° 289253 (REFINE project). Valerio Ferrario is grateful to MIUR (Ministero dell'Istruzione, dell'Università e della Ricerca - Roma) and to Università degli Studi di Trieste for financial support. Lucia Gardossi acknowledges EU COST Action CM1303 System Biocatalysis for financial support.

Notes and references

- 1 P. Ellwood, *J. Chem. Eng.* 1967, **74**, 98.
- 2 R. A. Gross, M. Ganesh and W. Lu, *Trends Biotechnol.* 2010, **28**, 435-443.
- 3 D. G. Barrett, T. J. Merkel, J. C. Luft and M. N. Yousof, *Macromolecules*, 2010, **42**, 9660-9667.
- 4 A. Pellis, L. Corici, L. Sinigoi, N. D'Amelio, D. Fattor, V. Ferrario, C. Ebert and L. Gardossi, *Green Chem.* 2015, **17**, 1756-1766.
- 5 L. Corici, A. Pellis, V. Ferrario, C. Ebert, S. Cantone and L. Gardossi, *Adv. Synth. Catal.*, 2015, **357**, 1763-1774.
- 6 H. Uyama, M. Kuwabara, T. Tsujimoto and S. Kobayashi, *Biomacromolecules*, 2003, **4**, 211-215.
- 7 S. Kobayashi, *Proc. Jpn. Acad., Ser. B* 2010, **86**, 338-365.
- 8 R. A. Gross, A. Kumar and B. Kalra, *Chem. rev.* 2001, **101**, 2097-2124.
- 9 B. Chen, J. Hu, E. M. Miller, W. Xie, M. Cai and R. A. Gross, *Biomacromolecules*, 2008, **9**, 463-471.
- 10 A. Mahapatro, B. Kalra, A. Kumar and R. A. Gross, *Macromolecules*, 2004, **37**, 35-40.
- 11 D. Feder and R. A. Gross, *Biomacromolecules* 2010, **11**, 690-697.
- 12 M. Hunsen, A. Azim, H. Mang, S. R. Wallner, A. Ronkvist, W. Xie and R. A. Gross, *Macromolecules* 2007, **40**, 148-150.
- 13 M. Hunsen, A. Azim, W. Xie and R. A. Gross, *Biomacromolecules*, 2008, **9**, 518-522.
- 14 M. Hunsen, A. Azim, H. Mang, S. R. Wallner, A. Ronkvist, W. Xie and R. A. Gross, *Polymer Preprints* 2006, **47**, 253.
- 15 A. Pellis, E. Herrero Acero, H. Weber, M. Obersriebnig, R. Breinbauer, E. Srebotnik and G. M. Guebitz, *Biotechnol. J.* 2015, DOI:10.1002/biot.201500074.
- 16 C. M. L. Carvalho, M. R. Aires-Barros and J. M. S. Cabral, *Electr. J. Biotechnol.* 1998, **1**, 160-173.
- 17 P. Sieber, M. Schorderet, U. Ryser, A. Buchala, P. Kolattukudy, J.-P. Métraux and C. Nawrath, *The Plant Cell* 2000, **12**, 721-737.
- 18 P. E. Kolattukudy, *Cutin from Plants*, Wiley, Biopolymers, 2005.
- 19 I. Borreguero, C. M. L. Carvalho, J. M. S. Cabral, J. V. Sinisterra and A. R. J. Alcantara, *J. Mol. Cat. B: Enzym.* 2001, **11**, 613-622.
- 20 C. M. L. Carvalho, M. R. Aires-Barros and J. M. S. Cabral, *Biotechnol. Bioeng.* 1999, **66**, 17-34.

- 21 D. P. C. de Barros, F. Lemos, L. P. Fonseca and J. M. S. Cabral, *J. Mol. Cat. B: Enzym.* 2010, **66**, 285–293.
- 22 D. P. C. de Barros, P. Fernandes, J. M. S. Cabral and L. P. Fonseca, *Catalysis Today* 2011, **173**, 95–102.
- 23 E. Stavila, R. Z. Arsyi, D. M. Petrovic and K. Loos, *Eur. Polym. J.* 2013, **49**, 834–842.
- 24 E. Stavila, G. O. R. A. Ekenstein and K. Loos, *Biomacromolecules* 2013, **14**, 1600–1606.
- 25 S. Liebming, A. Eberl, F. Sousa, S. Heumann, G. Fisher-Colbrie, A. Cavaco-Paulo and G. M. Guebitz, *Biocatal. Biotrans.* 2007, **25**, 171–177.
- 26 S. Yang, H. Xu, Q. Yan, Y. Liu, P. Zhou and Z. Jiang, *J. Ind. Microbiol. Biotechnol.* 2013, **40**, 217–226.
- 27 D. Ribitsch, E. Herrero Acero, K. Greimel, A. Dellacher, S. Zitzenbacher, A. Marold, R. D. Rodriguez, G. Steinkellner, K. Gruber, H. Schwab and G. M. Guebitz, *Polymers* 2012, **4**, 617–629.
- 28 D. Ribitsch, E. Herrero Acero, K. Greimel, I. Eiteljoerg, E. Trotscha, G. Freddi, H. Schwab and G. M. Guebitz, *Biocatal. Biotransform.* 2011, **30**, 2–9.
- 29 C. Martinez, P. De Geus, M. Lauwereys, G. Matthyssens and C. Cambillau, *Nature* 1992, **356**, 615–618.
- 30 L. D. Creveld, A. Amadei, R. C. van Schaik, H. A. Pepermans, J. de Vlieg and H. J. Berendsen, *Proteins* 1998, **33**, 253–264.
- 31 V. Ferrario, C. Ebert, L. Knapic, D. Fattor, A. Basso, P. Spizzo and L. Gardossi, *Adv. Synth. Catal.* 2011, **353**, 2466–2480.
- 32 V. Ferrario, L. Siragusa, C. Ebert, M. Baroni, M. Foscatto, G. Cruciani and L. Gardossi, *PLoS One* 2014, **9**, e109354.
- 33 E. Herrero Acero, D. Ribitsch, G. Steinkellner, K. Gruber, K. Greimel, I. Eiteljoerg, E. Trotscha, R. Wei, W. Zimmermann, M. Zinn, A. Cavaco-Paulo, G. Freddi, H. Schwab and G. M. Guebitz, *Macromolecules* 2011, **44**, 4632–4640.
- 34 D. Ribitsch, E. H. Acero, A. Przylucka, S. Zitzenbacher, A. Marold, C. Gamerith, R. Tscheließnig, A. Jungbauer, H. Rennhofer, H. Lichtenegger, H. Amenitsch, K. Bonazza, C. P. Kubicek, I. S. Druzhinina and G. M. Guebitz, *Appl. Env. Microbiol.* 2015, **81**, 3586–3592.
- 35 G. Cerea, L. Gardossi, L. Sinigoi and D. Fattor, World Patent WO/2013110446A1, 2013.
- 36 H. M. Berman, J. Westbrook, Z. Feng, G. Gilliland, T. N. Bhat, H. Weissig, I. N. Shindyalov and P. E. Bourne, *Nucleic Acids Res.* 2000, **28**, 235–242.
- 37 C. Roth, R. Wei, T. Oeser, J. Then, C. Follner, W. Zimmermann and N. Strater, *Appl. Microbiol. Biotechnol.* 2014, **98**, 7815–7823.
- 38 D. Kold, Z. Dauter, A. K. Laustsen, A. M. Brzozowski, J. P. Turkenburg, A. D. Nielsen, H. Koldso, E. Petersen, B. Schiott, L. De Maria, K. S. Wilson, A. Svendsen and R. Wimmer, *Protein Sci.* 2014, **23**, 1023–1035.
- 39 A. Basso, P. Braiuca, S. Cantone, C. Ebert, P. Linda, P. Spizzo, P. Caimi, U. Hanefeld, G. Degrassi and L. Gardossi, *Adv. Synth. Catal.* 2007, **349**, 877–886.
- 40 S. Cantone, P. Spizzo, D. Fattor, V. Ferrario, C. Ebert and L. Gardossi, *Chemistry Today* 2012, **30**, 22–26.
- 41 C. Mateo, R. Torres, G. Fernández-Lorente, C. Ortiz, M. Fuentes, A. Hidalgo, F. López-Gallego, O. Abian, J. M. Palomo, L. Betancor, B. C. C. Pessela, J. M. Guisan and R. Fernández-Lafuente, *Biomacromolecules* 2003, **4**, 772–777.
- 42 S. Cantone, V. Ferrario, L. Corici, C. Ebert, D. Fattor, P. Spizzo and L. Gardossi, *Chem. Soc. Rev.* 2013, **42**, 6262–6276.
- 43 P. Braiuca, A. Buthe, C. Ebert, P. Linda and L. Gardossi, *Biotechnol. J.* 2007, **2**, 214–220.
- 44 C. Korupp, R. Weberskirch, J. J. Müller, A. Liese and L. Hilterhaus, *Org. Proc. Res. Devel.* 2010, **14**, 1118–1124.
- 45 F. Binns, P. Harffey, S. M. Roberts and A. Taylor, *J. Chem. Soc., Perkin Transactions 1*, 1999, 2671–2676.
- 46 F. Binns, P. Harffey, S. M. Roberts and A. Taylor, *J. Polym. Sci., Part A: Polym. Chem.*, 1998, **36**, 2069–2080.
- 47 L. Gardossi, P. B. Poulsen, A. Ballesteros, K. Hult, V. K. Svedas, D. Vasic-Racki, G. Carrea, A. Magnusson, A. Schmid, R. Wohlgemuth and P. J. Halling, *Trends Biotechnol.* 2010, **28**, 171–180.
- 48 L. Sarda and P. Desnuelle, *Biochim. Biophys. Acta* 1958, **30**, 513–521.
- 49 R. Verger and G. H. D. Haas, *Ann. Rev. Biophys. Bioeng.* 1976, **5**, 77–117.
- 50 S. Longhi, A. Nicolas, L. Creveld, M. Egmond, C. T. Verrips, J. de Vlieg, C. Martinez and C. Cambillau, *Proteins* 1996, **26**, 442–458.
- 51 C. Martinez, A. Nicolas, H. Tilbeurgh, M. P. Egloff, C. Cudrey, R. Verger and C. Cambillau, *Biochemistry* 1994, **33**, 83–89.
- 52 C. Mateo, O. Abian, G. Fernandez-Lorente, J. Pedroche, R. Fernandez-Lafuente, J. M. Guisan, A. Tam and M. Daminati, *Biotechnol. Prog.* 2002, **18**, 629–634.
- 53 L. Bordoli, F. Kiefer, K. Arnold, P. Benkert, J. Battey and T. Schwede, *Nature Protocols* 2008, **4**, 1–13.
- 54 K. Okonechnikov, O. Golosova and M. Fursov, *Bioinformatics* 2012, **28**, 1166–1167.
- 55 M. A. Larkin, G. Blackshields, N. P. Brown, R. Chenna, P. A. McGettigan, H. McWilliam, F. Valentin, I. M. Wallace, A. Wilm, R. Lopez, J. D. Thompson, T. J. Gibson and D. G. Higgins, *Bioinformatics* 2007, **23**, 2947–2948.
- 56 S. E. Eisenberg, D. Komarony and M. R. Wall, *J. Mol. Biol.*, 1984, **179**, 125–142.
- 57 J. Uppenberg, M. T. Hansen, S. Patkar and T. A. Jones, *Structure*, 1994, **2**, 293–308.
- 58 T. J. Dolinsky, J. E. Nielsen, J. A. McCammon and N. A. Baker, *Nucleic Acids Res.* 2004, **32**, W665–667.
- 59 H. Li, A. D. Robertson and J. H. Jensen, *Proteins* 2005, **61**, 704–721.
- 60 G. A. Kaminski, R. A. Friesner, J. Tirado-Rives and W. L. Jorgensen, *J. Chem. Phys. Chem. B*, 2001, **105**, 6474–6487.
- 61 C. Caleman, P. J. van Maaren, M. Hong, J. S. Hub, L. T. Costa and D. van der Spoel, *J. Chem. Theory Comput.* 2012, **8**, 61–74.
- 62 B. Hess, C. Kutzner, D. v. d. Spoel and E. Lindahl, *J. Chem. Theory Comput.* 2008, **4**, 435–447.
- 63 U. Essmann, L. Perera, M. L. Berkowitz, T. Darden, H. Lee and L. G. Pedersen, *J. Chem. Phys.* 1995, **103**, 8577.
- 64 G. Bussi, D. Donadio and M. Parrinello, *J. Chem. Phys.* 2007, **126**, 014101.
- 65 H. J. C. Berendsen, J. P. M. Postma, W. F. van Gunsteren, A. Di Nola and J. R. Haak, *J. Chem. Phys.* 1984, **81**, 3684.

Table of contents:

Catalytic and structural properties make Cutinase 1 from *Thermobifida cellulosilytica* a more efficient biocatalyst for polycondensations, also of short-chain monomers.